

Wide field-of-view Schmidt-sphere imaging collimator

Berton C. Willard
MIT Lincoln Laboratory
244 Wood Street
Lexington, MA 02420-9185

ABSTRACT

A collimator was required to qualify the Advanced Land Imager (ALI) instrument of the EO-1 new millennium satellite for focus, MTF measurements, and distortion. It was used during assembly of the instrument and during thermal cycling while the instrument was in a vacuum tank. It had to be diffraction-limited over a 3 x 3 degree field of view and over a waveband of 400 to 2500 nm, have no obstruction, and have a virtual exit pupil that could be imaged onto the entrance pupil of the telescope. To satisfy these requirements the collimator, external to the vacuum tank, was built comprising a spherical mirror with exit pupil at its center of curvature, a full-aperture beamsplitter in collimated space, and a single lens to flatten the field. The optical layout and method of verifying collimation will be presented as well as optical performance, of interest since no corrector plate could be used as in the usual Schmidt camera configuration.

Key Words: EO-1, imaging collimator, Schmidt sphere.

1. INTRODUCTION

In order to verify the performance of the Advanced Land Imager (ALI) instrument of the EO-1 new millennium satellite, it was necessary to provide a wide-field collimator that could be used to project a scanning knife edge and a series of test patterns onto the ALI focal plane. The collimator was used first in a clean room to set the detector array to the instrument focal plane using shims. Second, the ALI instrument was placed in a thermal vacuum tank and the collimator was used to measure image performance. The collimator remained outside the vacuum tank.

The requirements for the collimator are given in Table 1.

Table 1:

Requirements For The Imaging Collimator.

- | | |
|-----------------------------|---|
| 1. collimated beam diameter | 12.5cm |
| 2. field-of-view | ± 1.6 degrees |
| 3. waveband | 0.4 to 2.5 micrometers. |
| 4. obstruction | none |
| 5. exit pupil location | at virtual entrance pupil of ALI instrument |
| 6. image quality | diffraction limited across a flat field |

These requirements could best be met with a collimator modeled after the Schmidt sphere, that is, with the aperture stop at the center of curvature of a spherical mirror. A field lens was added to flatten the field, and a beamsplitter added to eliminate the obstruction.

2. OPTICAL DESIGN

The optical layout for the imaging collimator is given in Figure 1. The insert shows the ALI instrument at the same scale. Its first three mirrors are powered, and the fourth is a fold flat. The secondary is the aperture stop, thus creating a virtual entrance pupil behind the primary mirror. The field of view in the plane of the drawing, which is also the direction of motion projected onto the earth's surface, is ± 0.628 degrees. Normal to the motion direction, the field is ± 7.5 degrees. The telescope was tested with the ± 7.5 degree field in the horizontal plane. While in the vacuum test chamber, the instrument could be swung in azimuth the full ± 7.5 degrees, but it could not be moved in elevation. Because of its field, however, the imaging collimator could image a target to anywhere in the 1.2 x 15 degree field.

From the entrance pupil of the ALI instrument on the left side of Figure 1 and tracing the system backward collimated light passes through the fused-silica vacuum-tank window, through the tilted fused-silica beamsplitter, reflects from the spherical mirror and beamsplitter, comes to focus just behind the field lens, and continues through a condensing lens, which images the entrance pupil onto the 2.54cm output port of an integrating sphere. Figure 2 shows more clearly the arrangement of the lenses, target plane, and integrating sphere port. A quartz-halogen lamp illuminated the sphere. The field lens is used to flatten the field of the spherical mirror. It turned out that with a 300cm radius of curvature on the spherical mirror its field curvature could be corrected with a stock plano-convex lens of 100cm focal length. The condenser lens was another stock plano-convex lens of 45cm focal length, both of BK-7 glass.

The center of curvature of the sphere was placed at the entrance pupil to the ALI telescope. Thus, neither coma nor astigmatism was created by the collimator.

The normal wide-field Schmidt camera requires an aspheric corrector plate at the aperture stop to correct spherical aberration, since it is a low F/number system. In the present application, the corrector plate could not be used because of the virtual entrance pupil of the ALI instrument. To avoid the need for a corrector plate the F/number was made large enough that spherical aberration was not a serious concern. F/12 was selected to match the 12.5cm diameter entrance pupil, resulting in the 300cm radius of curvature for the mirror mentioned above. Over the 12.5cm aperture and at best focus for 633 nm (minimum wavefront rms), the on-axis residual wavefront error is 0.055 waves p-v (0.017 waves rms), and 1.6 degrees off axis it is 0.068 waves p-v (0.018 waves rms). About half of the increase in wavefront error from on axis to 1.6 degrees off axis comes from a small amount of residual Petzval field curvature.

The imaging collimator bench layout is shown in Figure 3. The spherical mirror and beamsplitter can be seen on the left side of the optical bench; the lenses and integrating sphere are on the right. The beamsplitter was coated with inconel, such that the product of reflection and transmission was between 8 and 10 percent over the 0.4 to 2.5 micrometer bandwidth. Just to the right of the field lens was the collimator focus where a 1951 USAF Test Pattern was mounted on a X-Y-Z motorized stage. An edge between the metal coating and transparent pattern was used as a knife edge to set focus. It was then scanned across the focal plane to collect knife-edge scan data from the ALI detectors, which were then used to compute MTF data. The integrating sphere and condenser lens could be interchanged with a laser unequal path interferometer (LUPI) using locating stops. The LUPI was first used to check alignment between the field lens and spherical mirror and then to collimate the test pattern as will be explained later. The function of the black absorber to the left of the bench was to prevent light that first transmits the beamsplitter from scattering from objects in the room and then reflecting directly into the ALI instrument.

A photograph of the left half of the imaging-collimator bench is shown in Figure 4; the components may be identified from Figure 3. Part of the 10-cm shear plate can be seen through the beamsplitter, and to the left of the beamsplitter is the Maksutov telescope used to image the sheared beams through a lens and onto a CCD camera. The shear fringes are displayed on the video monitor to the right. The window to the vacuum chamber is seen to the left of the beamsplitter mount.

3. METHOD OF COLLIMATION

To assure that the collimator was projecting a collimated beam, a three step procedure was followed. First, the LUPI was placed on the optical bench using the locating stops. For this function the condensing lens and the integrating sphere, each with its own locating stops, were removed and the LUPI slid into position so as to be aligned to two irises that defined the optical axis of the collimator. The lenses impose an optical axis to the otherwise monocentric Schmidt sphere. The shear plate temporarily placed between the beamsplitter and vacuum tank window projected the axial portion of the collimator output beam into a Maksutov telescope and CCD camera to examine the shear fringes on the video monitor.

Typical shear fringes produced in this way are shown in Figure 5, those on the left for a collimated beam and those in the middle for a slightly defocused beam. The vertical dimension of the beam is limited by the 8.9cm clear aperture of the Maksutov telescope; the horizontal dimension is limited by the shear plate. The fringe pattern is missing from the center because of the obstruction in the Maksutov telescope. In the absence of aberration the fringes are straight. When the beam is collimated, the fringes are parallel to the wire set parallel to the edge of the wedge in the shear plate. With 3rd order spherical aberration the fringes would be "S" shaped, and at paraxial focus they would be parallel to the wire at the center and curved up and down at opposite ends. Over the 12.5cm beam diameter the spherical aberration is 0.22 waves p-v at paraxial focus for

633 nm light. Since spherical aberration in waves scales as the 4th power of the beam diameter, over the 10-cm shear plate tilted at 45 degrees the spherical aberration reduces to 0.014 wave of shear fringes. This amount of spherical aberration is not discernable, so setting the ends of a fringe equi-distant from the wire assures that the LUPI beam has been set for paraxial focus.

Once the LUPI was producing a collimated beam, the second step could be performed. An edge in the test pattern was made to intercept the beam, and visual inspection of the cutoff shadow was used to set the edge at the LUPI focus. The test pattern was then transmitting a collimated target.

The final step was to set the test pattern at the best focus of the F/12 sphere, defined as that focus for minimum rms wavefront error at 633 nm as computed by OSLO PRO.

To provide a second test for collimation, a 15-cm diameter flat mirror with approximately 0.10 wave of power (wavefront) was put in place of the shear plate and set to reflect the LUPI beam back upon itself, thus producing LUPI fringes that could be examined on a video monitor and compared to the shear fringes. On the right side of Figure 5 is a LUPI interferogram taken over the 15-cm aperture with the same focus as the collimated shear plate setting on the left. Focus uncertainty will be discussed in Section 5.

4. DISTORTION

The field lens introduced a small amount of distortion to the collimator. For example, at the maximum field angle of 1.6 degrees, the angular distortion ranged between 20 and 16 microradians depending upon the waveband, as computed by OSLO PRO. This was a small fraction of the ALI distortion, but nevertheless it was accounted for in the measurement of the ALI distortion. Distortion was measured by projecting a square-wave Ronchi grating of known frequency onto the ALI focal plane. Distortion could be measured only over that part of the ALI focal plane which was populated with detector arrays, centered 6.0 degrees off axis in the cross flight direction and on axis in the flight direction. A more detailed discussion of distortion measurement can be found in SPIE conference paper 3750-13.

5. FOCUS UNCERTAINTY

The contributors to focus uncertainty are included in Table 2 below.

The primary reference for focusing the imaging collimator was a 10-cm aperture shear plate. The shear plate calibration was checked with a Zygo interferometer showing fringes between the front and rear surface. To check the parallelism of the fringes to the wire one makes two estimates of fringe-wire spacing, one on each end of the fringe. It was calculated that with the given shear plate the uncertainty in the wavefront curvature due to these two estimates was 0.16 waves p-v, scaled to the F/7.5 aperture of the ALI telescope, for the first entry in Table 2.

Collimation with the shear fringes was performed by examining the fringe pattern on the camera monitor, which appeared as in Figure 4. The value above, 0.16 waves p-v, was again used for entry number 2.

The second step in collimation was setting the knife edge to focus using the cutoff shadow from the LUPI source. This was also a test of the LUPI objective, and there was no visual indication of uneven cutoff at focus. Repeatability of this subjective test was checked by making a series of readings of the axial position of the knife edge using the motorized focus stage when it appeared to give perfect cutoff. The maximum spread for 10 readings was 13 micrometers. Over the F/8 cone of the LUPI objective, this spread corresponded to a defocus of 0.026 micrometers, which was then scaled to 0.036 waves p-v for the F/7.5 aperture of the ALI instrument, for entry number 3.

The fourth entry is for residual power in the vacuum window, which was 0.049 waves p-v as measured with a Zygo interferometer.

The fifth entry in Table 2 dealt with the orthogonality between the collimator axis and the motorized cross slide carrying the knife edge test pattern. The shear plate was used to collimate the LUPI beam, and the knife-edge was set at cutoff at a series of focus positions across the ± 1.6 degree field in both azimuth and elevation. The cross slide was adjusted until a straight line fit to the data points gave a maximum deviation of 0.030 waves p-v for the shear plate defocus across the field. In order to perform this setup, it was necessary to place the shear plate at the center of curvature of the spherical mirror, because of the residual spherical aberration, so that the shear plate collimated the center of the beam for each field point.

The last entry in Table 2 allowed for the axial chromatic aberration introduced by the field lens since the knife edge scans across all ALI wavebands were taken with one focus setting. Possible defocus from thermal expansion of the optical bench was avoided by focusing the collimator before every set of data taken.

The resulting rss value of 0.23 waves p-v corresponded to an axial defocus uncertainty in the ALI instrument of 0.0026 inches (units chosen to match the specifications).

Table 2
Focus Uncertainty For Imaging Collimator
 Values are waves p-v for the F/7.5 aperture of the ALI instrument,
 and at 633 nm

1.	Shear plate calibration	0.16	
2.	Shear plate reading	0.16	
3.	Knife edge focus	0.036	
4.	Vacuum window power	0.049	
5.	Shear plate defocus across field	0.030	
6.	Across waveband defocus	0.036	
	rss	0.23 waves p-v	
	Axial defocus in ALI instrument	0.0026 inch.	

The operational focus error budget for the ALI instrument allowed a total system focus error of ± 0.003 inch but there was nothing allowed for the imaging collimator, although there was a contingency of ± 0.001 inch. If this contingency is replaced with the imaging collimator focus uncertainty the total system focus error becomes ± 0.0038 inch, just over budget.

6. NON-FOCUS WAVEFRONT ERROR

The random wavefront error in the imaging collimator from its separate components is summarized in Table 3. The values are from measurements with a Zygo interferometer. Measurements of the field lens were not included, since it was so close to the image plane, about 0.3 cm from the plane side. The residual spherical aberration at best focus, as computed by OSLO PRO, was added to the table as item 6. Including the nominal design, the total wavefront error is estimated to be 0.26 waves p-v and 0.05 waves rms at 0.632 micrometers across the field and for the F/7.5 aperture of the ALI instrument.

Table 3
Non-focus Wavefront Error Estimate For Imaging Collimator
 Values are waves p-v for the F/7.5 aperture of the ALI instrument,
 and at 0.632 micrometers.

1.	Vacuum window	0.05	
2.	Beamsplitter in reflection	0.20	
3.	Beamsplitter in transmission	0.12	
4.	Spherical mirror	0.08	
5.	Field lens	not measured	
6.	Nominal design	0.055 at best focus on axis	
		0.068 1.6 degrees off axis	
			rss 0.26 waves p-v
		0.05 waves rms	
		on axis and 1.6 degrees off axis.	

7. IMPROVEMENTS

The biggest improvement to the imaging collimator would be to reduce the focus uncertainty. Since the largest contributor to the focus uncertainty is the shear plate, as seen in Table 2, going to a larger shear plate would be beneficial. For example, it is estimated that by switching from a 100 millimeter to a 150 millimeter shear plate the values for shear plate calibration and reading in Table 2 would be reduced to about 0.09 waves p-v, reducing the ALI focus uncertainty to about ± 0.0016 inch. Autocollimating a LUPI from a reference flat instead of using the shear plate may not necessarily lead to reduced uncertainty. For example, using a reference flat with surface power of 1/20 p-v would lead to roughly the same uncertainty as in Table 2, considering the uncertainty in measuring the reference flat and reading the LUPI fringes.

8. CONCLUSIONS

The feasibility of using a Schmidt sphere as a wide flat-field broadband collimator with no central obstruction has been demonstrated. By using a 10-centimeter aperture shear plate the collimation uncertainty over a 12.5 centimeter aperture and across a ± 1.6 degree field was 0.23 waves p-v.

ACKNOWLEDGMENTS

The author wishes to thank Frank Perry for his help in initially assembling the collimator and then moving it to the clean room and reassembling and aligning the components.

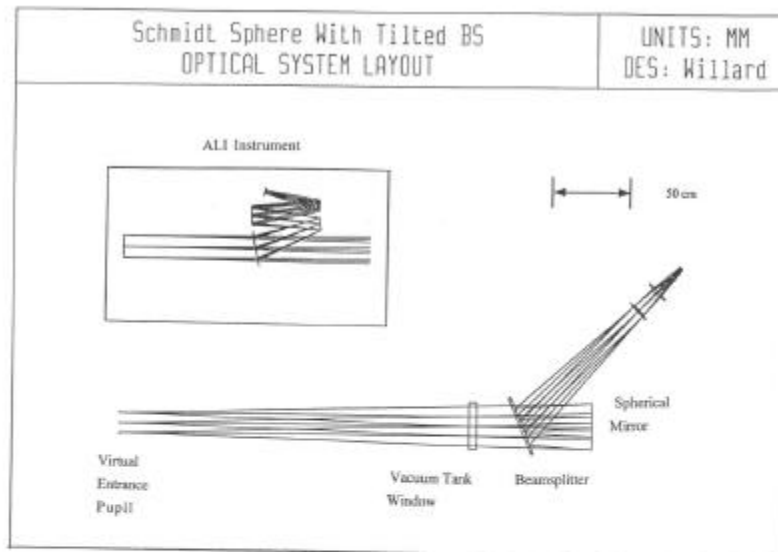


Fig. 1. Raytrace of imaging collimator. Insert: Raytrace of the ALI telescope to the same scale as the imaging collimator.

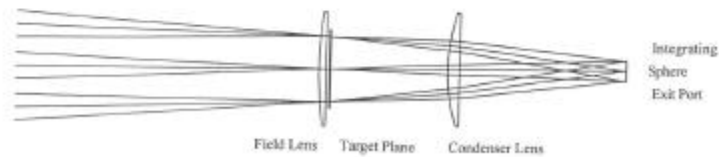


Fig. 2. Enlarged section of Fig. 1 showing field lens, target plane, condenser lens, and integrating sphere exit port.

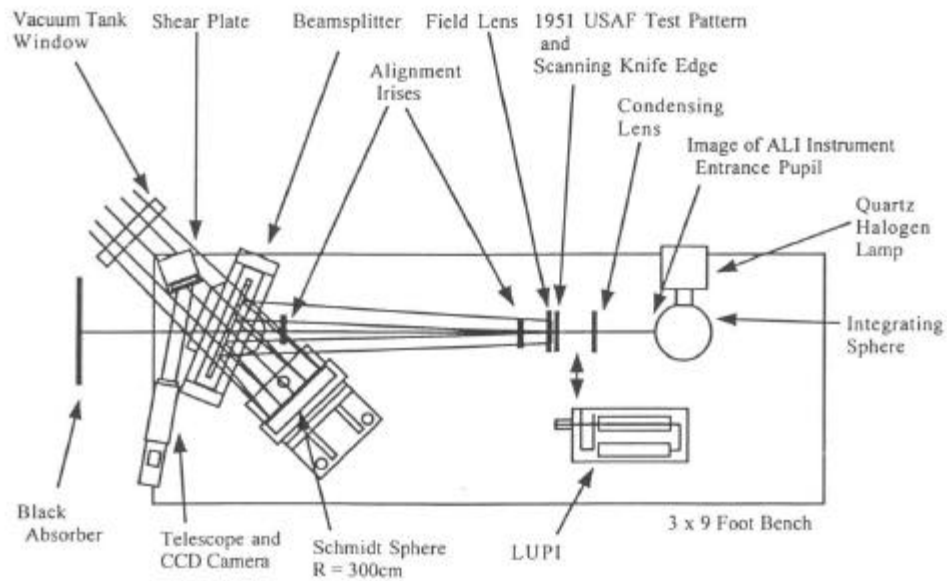


Fig. 3. Optical Layout of the ALI Imaging Collimator.

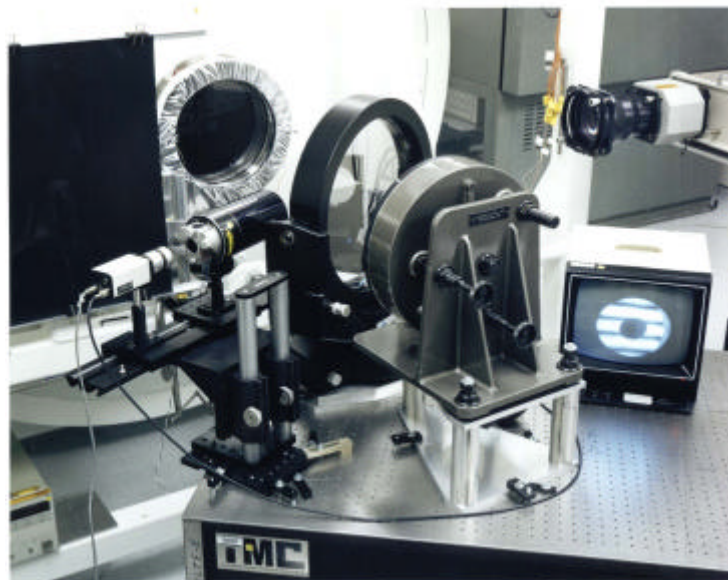


Fig. 4. Photograph of the left side of the optical bench holding the ALI Imaging Collimator as shown in Fig. 3.

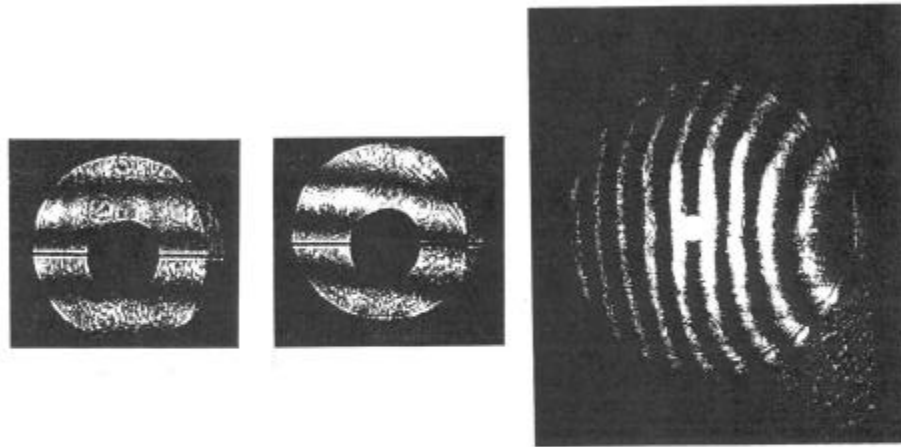


Fig. 5 Left: shear fringes indicating collimation. Middle: shear fringes showing defocus. The vertical clear aperture is limited to 8.9 cm; the horizontal clear aperture is limited by the 10 cm shear plate at a 30-degree incident angle. Right: LUPI fringes at the same focus setting as the collimated shear fringes on the left. The clear aperture is 15 cm.